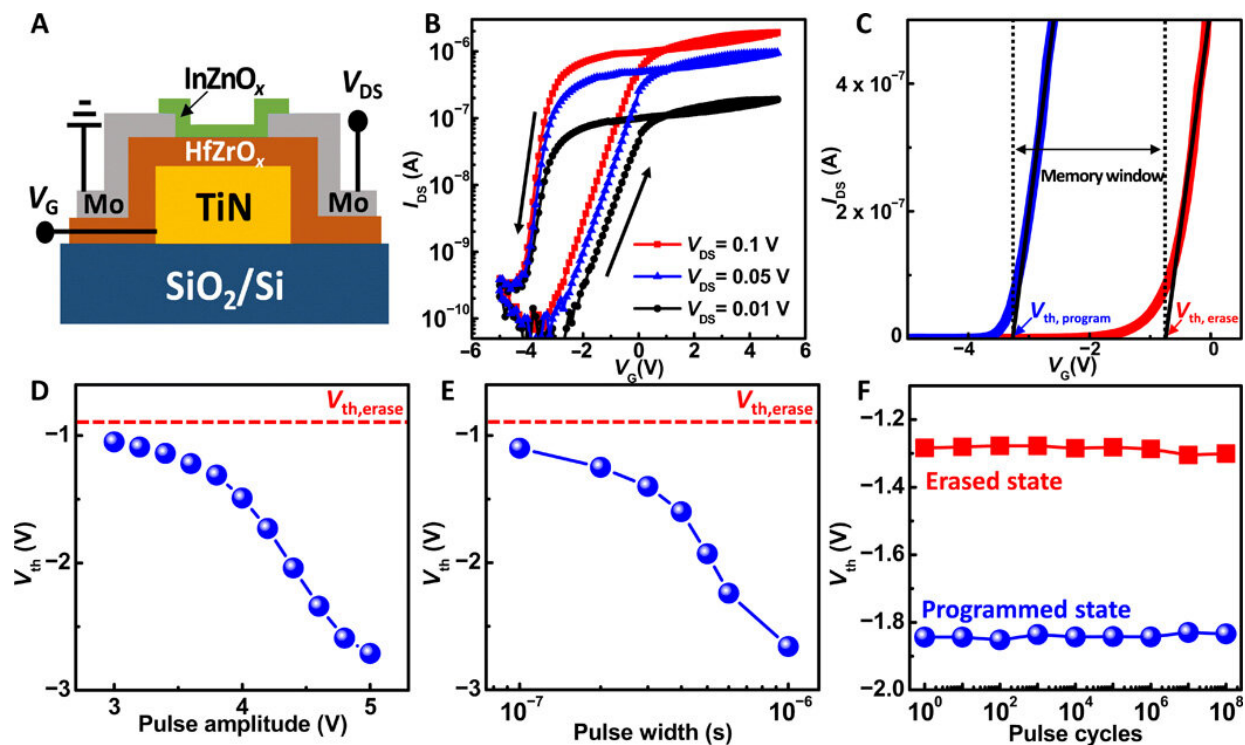


High-speed 3-D memory with ferroelectric NAND flash memory

January 26 2021, by Thamarasee Jeewandara



FeTFT for nonvolatile memory applications. (A) Schematic illustration of FeTFT that uses HfZrOx and InZnOx. (B) Transfer curves of FeTFT with $V_{DS} = 0.1, 0.05,$ and 0.01 V. (C) I_{DS} - V_G curves of FeTFT in erased and programmed states. Threshold voltage V_{th} is extracted using the linear extrapolation. A memory window is the difference between erased and programmed V_{th} of FeTFT. V_{th} change of FeTFT according to (D) amplitudes and (E) widths of program pulses. In operation with different pulse amplitudes, pulse amplitudes are increased from 3 to 5 V and a width is fixed at 1 μ s. In operation with different pulse widths, pulse widths are increased from 100 ns to 1 μ s and an amplitude is fixed at 5 V. (F) Endurance characteristics of FeTFT

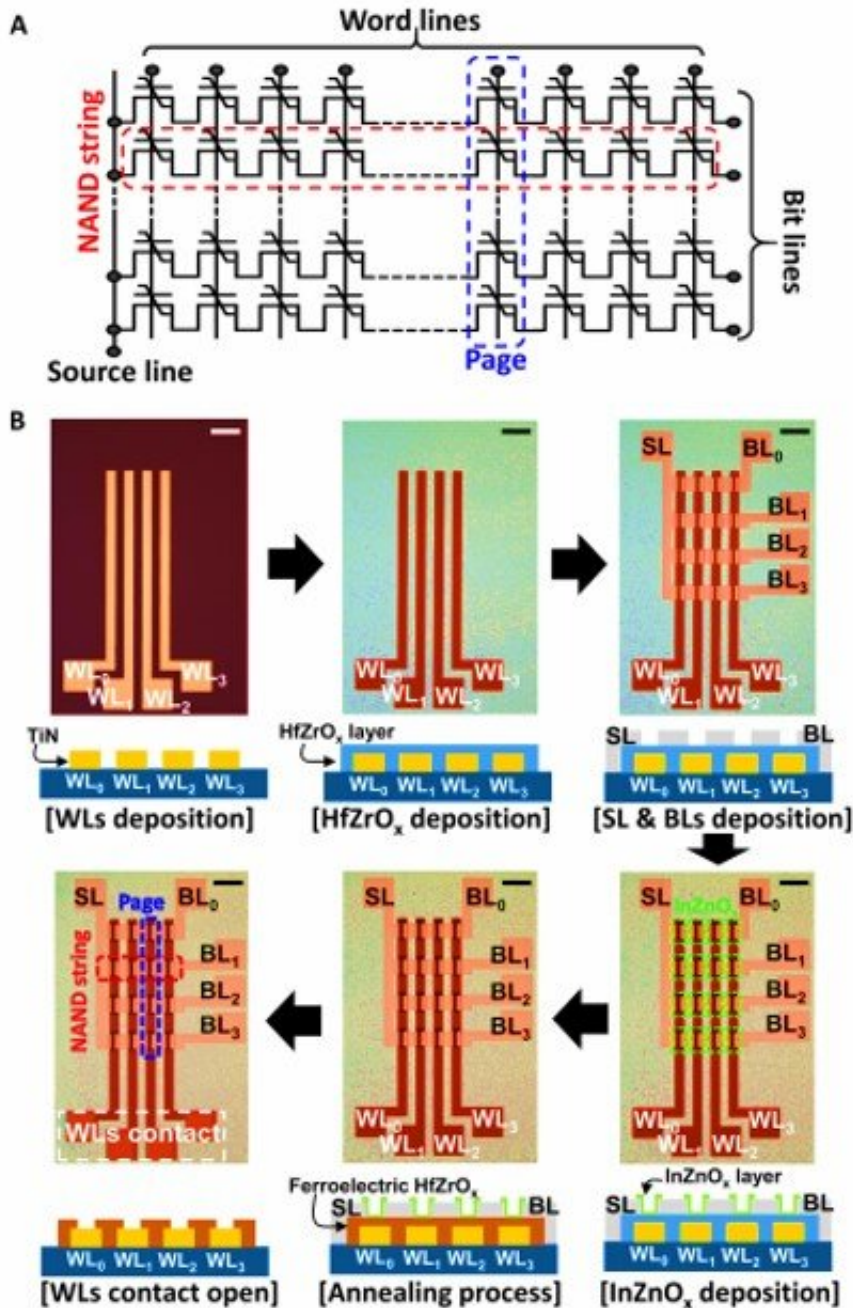
for 108 cycles using positive (5 V, 500 ns) and negative (−7 V, 1 μs) triangular pulses for program and erase operations, respectively. Credit: Science Advances, doi: 10.1126/sciadv.abe1341

Ferroelectric memory is a well-researched topic in the past decade due to its capacity for higher speed, lower power consumption and longer endurance, compared to conventional [flash memory](#). The performance of ferroelectric memory can be compromised substantially due to the formation of unwanted interfacial layers during the development of ferroelectric memory-based on perovskite oxides-on-silicon. In a new report, Min-Kyu Kim, and a team of scientists in materials science and engineering at the Pohang University of Science and Technology in Korea, demonstrated a unique strategy by applying [hafnia-based ferroelectrics](#) and oxide semiconductors for three-dimensional (3-D) integration. The strategy achieved memory performance beyond the conventional flash memory and exceeded those achieved by perovskite ferroelectric memories. The team then simulated the devices to confirm the ability to realize ultra-high-density 3-D memory integration.

Flash memory

Flash memory devices are presently in use for massive data storage across [mobile devices](#) and servers through [floating-gates](#) or [charge-trap memory transistors](#) based on [electron-tunneling through a tunnel oxide](#). The electron-tunneling process requires voltage pulses with high amplitude and long duration; however, [existing flash memory devices](#) only possess a high functional voltage approximating 20 volts and a slow speed coupled with limited endurance. The process further required high deposition and annealing temperatures to [form channel and oxide layers](#). Scientists therefore developed a range of emerging memory devices to

overcome these limits, however, there are [no existing alternatives to current flash memory](#) in order to obtain fast functionality at a low power. In the meantime, researchers have developed hafnia-based ferroelectric materials due to their complementary metal-oxide semiconductor (CMOS) compatibility, low power consumption and [fast switching speed](#).



Fabrication process of FeNAND array. (A) FeNAND memory array structure including word lines (WLs), bit lines (BLs), source line (SL), NAND strings, and pages. (B) Optical images and schematic illustrations of fabrication processes for 4×4 FeNAND flash memory array (scale bar: 100 μm). 4×4 FeNAND flash memory array consists of four pages and four NAND strings. ALD (atomic-layer deposition) is used for deposition of HfZrO_x and InZnO_x layer. Memory array consists of 16 memory cells. Credit: Science Advances, doi: 10.1126/sciadv.abe1341

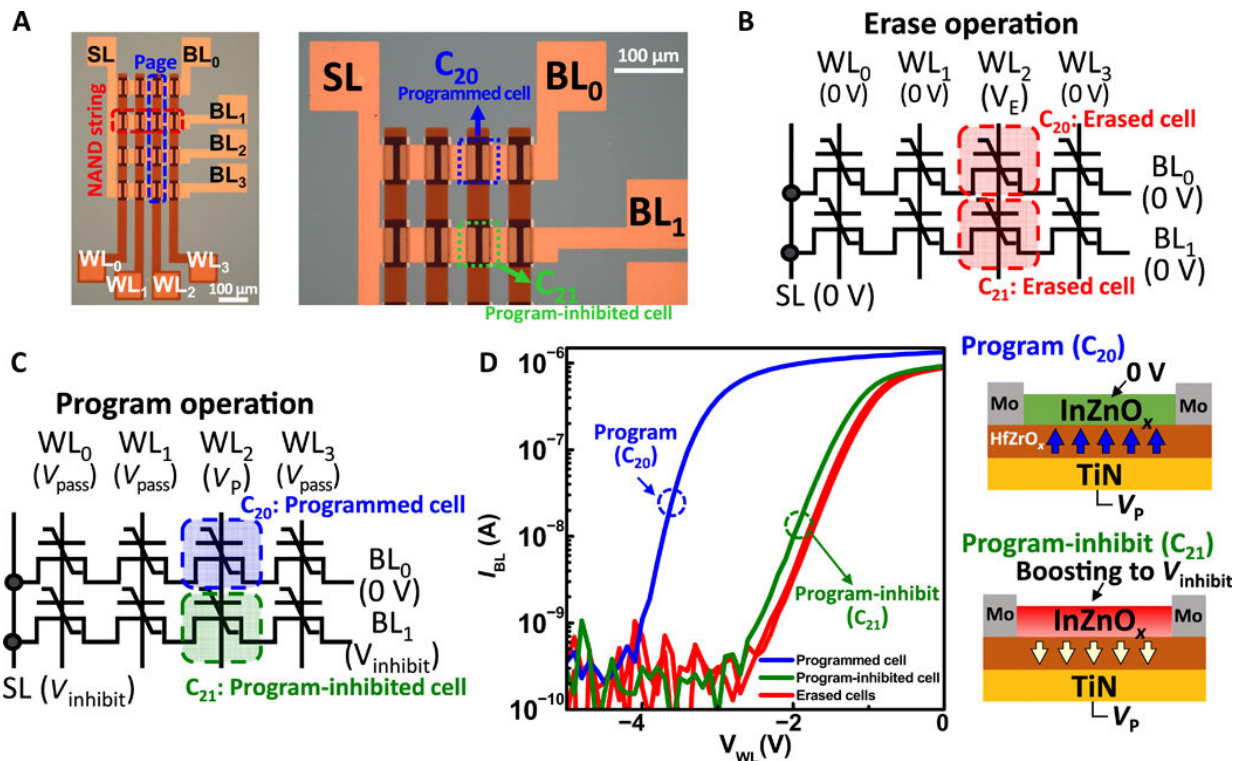
Kim et al. presented unique methods to overcome key issues of [ferroelectric memory](#) transistors by introducing [indium zinc oxide](#) (InZnO_x) as the semiconductor layer and [zirconium-doped hafnium oxide](#) (HfZrO_x) as the ferroelectric layer to obtain high-performance memories. The outcomes resulted in an operational speed several hundred times faster, and an operational voltage four times lower [compared to existing flash memory](#). All processes could be conducted below 400 degrees Celsius with integrated ferroelectric memory devices that are CMOS compatible to achieve commercialization milestones including [NAND \(NOT-AND gate\)](#) flash arrays and 3-D vertical structures. The nanoscale 3-D vertical flash memory showed excellent performances for ultra-high-density 3-D flash memory in the future.

Developing a high-performance ferroelectric transistor

Kim et al. first confirmed the ferroelectric properties of zirconium-doped hafnium oxide by developing a capacitor with a titanium nitride/zirconium-doped hafnium oxide/ titanium nitride ($\text{TiN}/\text{HfZrO}_x/\text{TiN}$) structure, and measured the [polarization-electric field](#) characteristics of the 24-nm thick material. The [coercive electric field](#) of the material was larger than that of ferroelectric [perovskite oxides](#) and advantageous in ferroelectric transistors since the large coercive electric fields comparatively led to [a larger memory window](#). The team next confirmed the ferroelectricity of zirconium-doped hafnium oxide using [piezoresponse force microscopy](#) and capacitance-voltage measurements to confirm their ferroelectric nature for endurance characteristics. The scientists tested the feasibility of the integration strategies using [ferroelectric thin-film transistors](#) (FeTFTs) with a bottom-contact structure developed using atomic layer deposition-based zirconium-doped

hafnium oxide and indium zinc oxide (HfZrO_x and InZnO_x). To confirm the reliability of these ferroelectric thin-film transistors, Kim et al. also tested their endurance properties. The robust endurance character of the setup originated from its metal-ferroelectric semiconductor structure without an interfacial layer. Compared to previous memory devices such as [charge-trap memory](#) and perovskite oxide-based ferroelectric transistors, the use of HfZrO_x and InZnO_x resulted in lower functional voltage, faster operation speed and lower processing temperature.

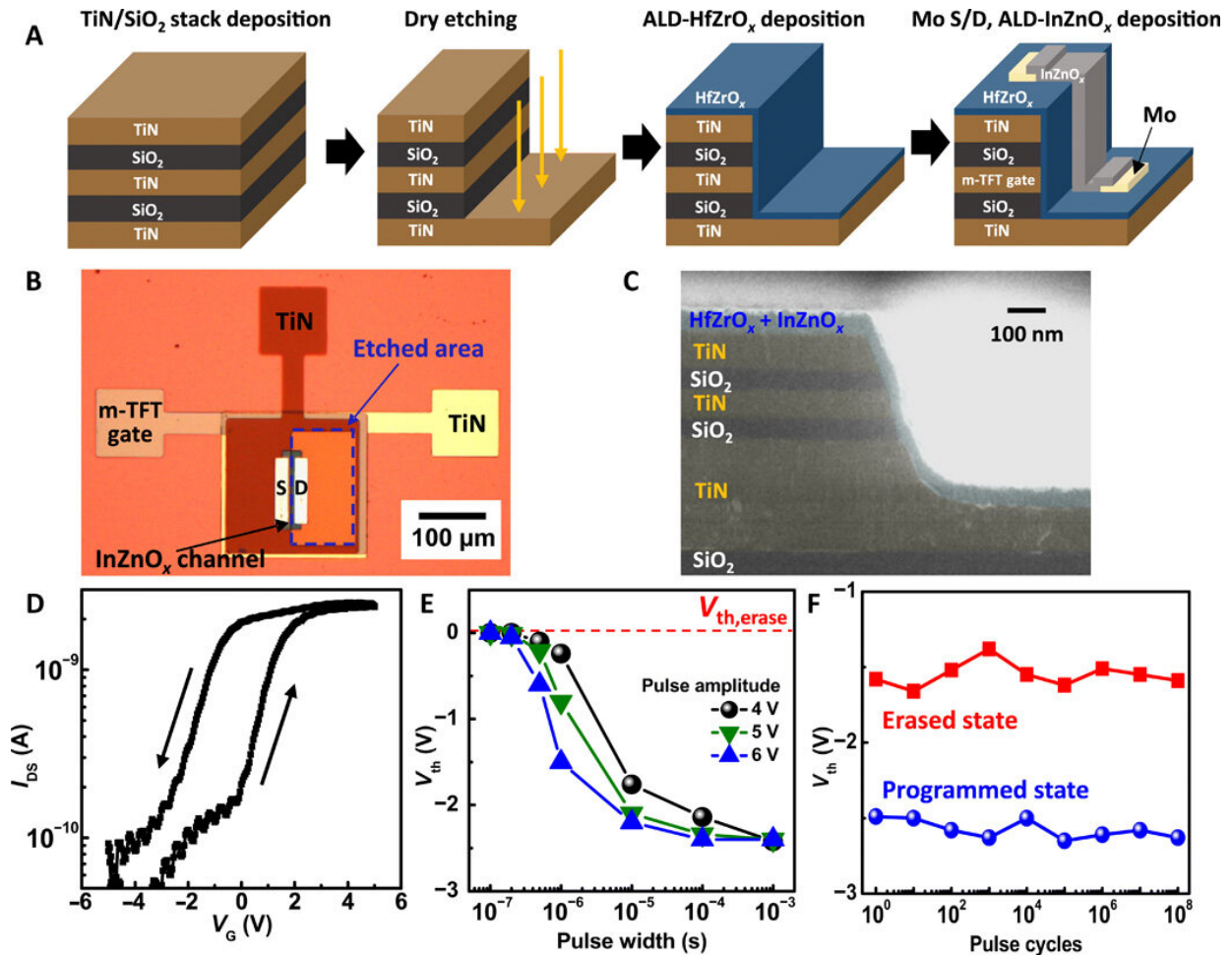
Memory operation of integrated ferroelectric NAND



Operation characteristics of FeNAND. (A) Optical image of 4×4 FeNAND flash memory array (left) and NAND strings in FeNAND flash memory array including programmed cell (C_{20}) and program-inhibited cell (C_{21})

(right). (B and C) Equivalent circuits of FeNAND flash memory array and erase/program operations. V_P , V_E , V_{pass} , and $V_{inhibit}$ stand for program, erase, pass, and inhibit voltages, respectively. (D) IBL-VWL curves of C20 memory cell and C21 memory cell after erase and program operations. Program of C21 memory cell is prevented by program-inhibit operation. Program-inhibit pulse with an amplitude of $V_{inhibit} = 2.5$ V is used for program-inhibit operation. During program-inhibit operation, the channel potential of C21 memory cell could be boosted to $V_{inhibit}$. Credit: Science Advances, doi: 10.1126/sciadv.abe1341

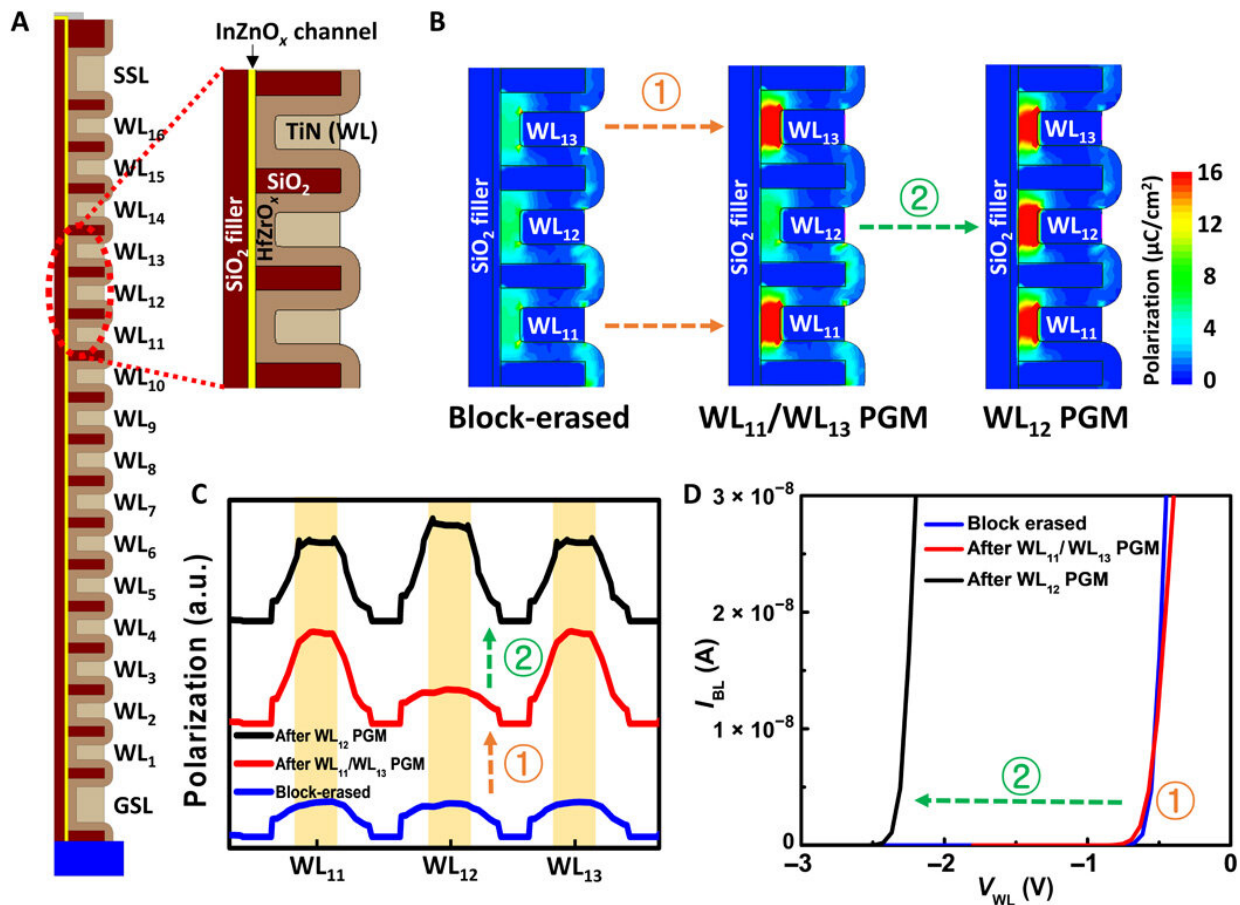
Flash memory cells are generally connected in a hierarchy to allow efficient access. Typically, a number of cells are connected in a string, organized in blocks, where each string in the block is connected to a separate [bitline](#) (BL) and the control gate of each cell in the string can be connected to a [wordline](#) (WL). Structurally, ferroelectric NAND (FeNAND) flash memory arrays are similar to NAND flash devices, while differing only by the type of memory cells. For example, FeNAND flash memory arrays typically use ferroelectric transistors, while NAND flashes used conventional flash memory. All FeNAND strings shared a [source line](#) (SL), while each NAND string was connected to bitlines. The team developed a 4 by 4 FeNAND array by including ferroelectric thin-film transistors with a ferroelectric zirconium-doped hafnium oxide layer and indium zinc oxide channel layer in a CMOS compatible fabrication process.



Nanoscale vertical FeTFT array. (A) Fabrication process flow for vertical FeTFT array. (B) Optical image of the vertical FeTFT device array. S and D stand for source and drain, respectively. (C) Cross-sectional scanning electron microscope image (false colors) of the vertical FeTFT array. (D) Transfer curve of m-TFT with counterclockwise hysteresis. For characterization, V_G sweep is applied to m-TFT gate electrode, while $V_{pass} = 1$ V is applied to unselected gate electrodes. (E) V_{th} change of m-TFT device according to program pulse amplitudes and widths. (F) Endurance characteristics of m-TFT device for 108 cycles using positive (6 V, 1 μs) and negative (-7 V, 1 μs) triangular pulses for program and erase operations, respectively. Credit: Science Advances, doi: 10.1126/sciadv.abe1341

The completed NAND array contained 16 memory cells to

demonstrate its program operation. Program disturbances could occur in the setup if unwanted programming occurred in memory cells during operation. To avoid this phenomenon, Kim et al. used a program-inhibit operation method by applying a program-inhibit pulse. During the experiments, all 16 memory cells in the FeNAND array functioned without fail and the results confirmed NAND memory operation to be successful with an array of ferroelectric thin-film transistors (FeTFTs). The team also developed FeNAND arrays on a silicon wafer and measured the program and erase operation of nine memory cells, where the experimental results and those simulated with the [technology computer-aided design \(TCAD\) tool](#) agreed with each other.



Device simulation of 3D FeNAND. (A) Device structure of simulated 3D FeNAND. A single string containing 16 WLs, ground select line (GSL), and string select line (SSL) is simulated. The 30-nm-thick TiN, 24-nm-thick HfZrO_x, and 10-nm-thick InZnO_x are used as WL, ferroelectric gate insulator, and oxide semiconductor channel, respectively. SiO₂ is used as oxide filler material. The thickness of SiO₂ spacer between adjacent WLs is 30 nm. (B) Simulated polarization in HfZrO_x layer after block-erase and program operations. First, all WLs are erased by block-erase operation. Then, WL11 and WL13 cells are programmed. Last, WL12 cell is programmed. Polarization in HfZrO_x layer is clearly changed after block-erase and program operations. (C) Polarization change after block-erase and program operations. a.u., arbitrary units. (D) IBL-VWL curves in WL12 cell after block-erase and program operations. Credit: Science Advances, doi: 10.1126/sciadv.abe1341

Simulating 3-D FeNAND devices

In order to understand the feasibility of ferroelectric thin-film transistors based on zirconium-doped hafnium oxide and indium zinc oxide within future 3-D FeNAND devices, Kim et al. then simulated a single string containing 16-word lines, a string select line and a ground select line. The team thereafter performed block-erase operations to further observe the operation characteristics of the 3-D FeNAND device. In this way, the 3-D FeNAND devices were successfully programmed with highly stacked structures to show that their constituent ferroelectric thin-film transistors maintained low power consumption and fast operation speed to replace 3-D NAND flash memory.

Min-Kyu Kim and colleagues demonstrated a combined ferroelectric [oxide](#) semiconductor channel as a unique integration strategy to solve key issues in ferroelectric memory transistors. They tested the potential of the ferroelectric memory as an alternative to conventional flash memory using an integrated FeNAND (ferroelectric NAND) and a

vertical ferroelectric thin-film transistor (FeTFT) array. The FeTFTs were functional in the vertical structure and the team confirmed the operation mechanisms via device simulation. They also confirmed the possibility of ultra-high density 3-D memory integration by simulating program and block-erase operational functions in 3-D FeNAND cells. The results suggested the atomic-layer deposition-based FeTFTs to have promising applications in future high-density 3-D [memory](#) devices.

More information: Kim M-K. et al. CMOS-compatible ferroelectric NAND flash memory for high-density, low-power, and high-speed three-dimensional memory, *Science Advances*, [DOI: 10.1126/sciadv.abe134](https://doi.org/10.1126/sciadv.abe134)

Lee C-H. et al. Charge-trapping device structure of SiO₂/SiN/high-k dielectric Al₂O₃ for high-density flash memory. *Applied Physics Letters*, doi.org/10.1063/1.1897431

Cheema S. S. et al. Enhanced ferroelectricity in ultrathin films grown directly on silicon, *Nature*, doi.org/10.1038/s41586-020-2208-x

© 2021 Science X Network

Citation: High-speed 3-D memory with ferroelectric NAND flash memory (2021, January 26) retrieved 12 August 2024 from <https://techxplore.com/news/2021-01-high-speed-d-memory-ferroelectric-nand.html>

This document is subject to copyright. Apart from any fair dealing for the purpose of private study or research, no part may be reproduced without the written permission. The content is provided for information purposes only.